

Extreme close encounters between proto-Mercury and proto-Venus in terrestrial planet formation

Tong Fang,¹ Hongping Deng,²★

¹ Center of Deep Sea Research, Institute of Oceanology, Chinese Academy of Sciences, Qingdao 266071, China

² Department of Applied Mathematics and Theoretical Physics, University of Cambridge, Centre for Mathematical Sciences, Wilberforce Road, Cambridge CB3 0ET, UK

25 August 2020

ABSTRACT

Modern models of terrestrial planet formation require solids depletion interior to 0.5–0.7 au in the planetesimal disk to explain the small mass of Mercury. Earth and Venus analogues emerge after ~100 Myr collisional growth while Mercury forms in the diffusive tails of the planetesimal disk. We carried out 250 N-body simulations of planetesimal disks with mass confined to 0.7–1.0 au to study the statistics of close encounters which were recently proposed as an explanation for the high iron mass fraction in Mercury by Deng (2020). We formed 39 Mercury analogues in total and all proto-Mercury analogues were scattered inward by proto-Venus. Proto-Mercury typically experiences 6 extreme close encounters (closest approach smaller than 6 Venus radii) with Proto-Venus after Proto-Venus acquires 0.7 Venus Mass. At such close separation, the tidal interaction can already affect the orbital motion significantly such that the N-body treatment itself is invalid. More and closer encounters are expected should tidal dissipation of orbital angular momentum be accounted. Hybrid N-body hydrodynamic simulations, treating orbital and encounter dynamics self-consistently, are desirable to evaluate the degree of tidal mantle stripping of proto-Mercury.

Key words: Terrestrial planets, Mercury, Close encounter

1 INTRODUCTION

The terrestrial planets in our solar system form through collisional growth between planetesimals embedded in a protoplanetary disk (Safronov 1969). The growth of dust to planetesimals under the influence of turbulence in protoplanetary disks remains elusive (see, e.g., review by Testi et al. 2014). The later collisions between planetesimals are readily modeled with N-body simulations (Kokubo & Ida 1998, 2000; Chambers & Wetherill 1998; Morishima et al. 2010). Earth and Venus analogues naturally emerge in N-body simulations (O’Brien et al. 2006) while replicating the smaller planets, Mars and Mercury remains challenging (Raymond et al. 2009). Recent model starting from planetary embryos confined between 0.7–1 au successfully produced Mars and Mercury analogues from material gravitationally scattered (diffused) outside the original annulus (Hansen 2009). The initial narrow annulus may be caused by the migration of Jupiter and Saturn in the protoplanetary disk (Walsh et al. 2011) or it can be intrinsic to the planetesimal distribution due to dust drift in protoplanetary disks (Drazkowska et al. 2016; Raymond & Izidoro 2017). The narrow annulus model and its variations are promising with high success rate in

replicating Mars and Mercury (Hansen 2009). Alternatively, an eccentric Jupiter (likely caused by giant planet instability, see Clement et al. 2018) can excite the planetesimal disk and form small Mars analogues.

The formation of Mercury, is arguably the most challenging problem in these N-body simulations (Lykawka & Ito 2017; Clement et al. 2019). To replicate the small mass of Mercury, an *ad hoc* depletion of solids interior to 0.5–0.7 au is typically invoked (see, e.g., Chambers 2001; Hansen 2009; Walsh et al. 2011; Clement et al. 2018) except in the in situ formation model of Lykawka & Ito (2017, 2019). The solids may be depleted by a massive body which later moved away, e.g., a super-Earth lost to Sun (Batygin & Laughlin 2015) or the Jupiter core migrated outwards (Raymond et al. 2016). The solids deficit can also be caused by the loss of early formed embryos to Sun (Ida & Lin 2008) or by the imprint of the fossil silicate snowline (Morbidelli et al. 2016). In these models, Mercury itself or its building blocks must be scattered inward 0.5 au. If the former is the case then violent encounters between proto-Mercury and proto-Venus may be necessary to kick proto-Mercury in.

Mercury also stands out for its anomalously high-iron mass fraction, 70% of the planet mass (Anderson et al. 1987; Hauck et al. 2013) while all other terrestrial planets have only 30% iron by mass. This rocky material deficit may be a re-

★ E-mail:hd353@cam.ac.uk

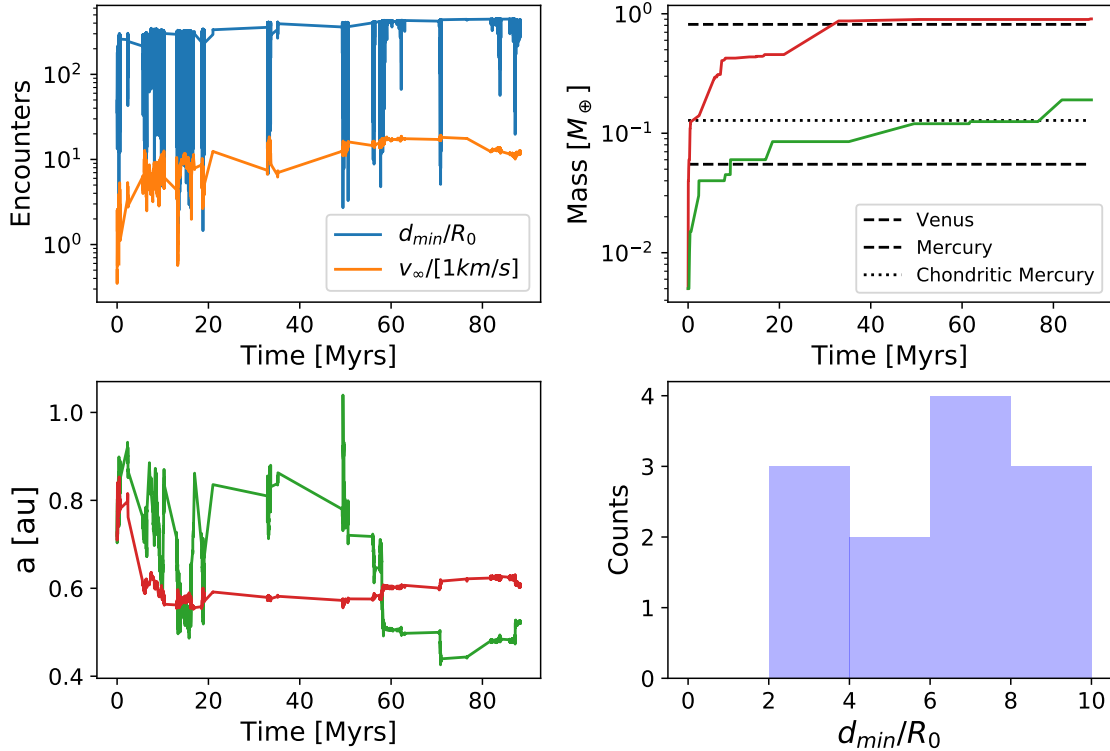


Figure 1. Encounters between proto-Mercury and proto-Venus in an exemplary simulation. *Upper left:* the closest approach d_{min} in the units of Venus radius, R_0 and the relative velocity at infinity v_{∞} for all the close encounter between the formed Mercury and Venus analogues. *Upper right:* mass growth of Mercury and Venus analogues. *Lower left:* semi-major axis of proto-Mercury and proto-Venus at the time of their close encounters. *Lower right:* the number of major encounters with d_{min} smaller than $10R_0$ (see text)..

sult of mantle removal due to giant impacts (Benz et al. 2008; Asphaug & Reufer 2014; Chau et al. 2018) or extreme close encounters with proto-Venus (Deng 2020). The high-temperature giant impact scenario seems at odds with the retainment of moderately volatile elements on the present-day Mercury (Peplowski et al. 2011). The multiple encounters scenario avoids high-temperature collisions but whether such extreme close encounters occur repeatedly remains uncertain. Deng (2020) shows mantle removal occurs for a non-spinning proto-Mercury passing by proto-Venus within 2 Venus radii. Although a prograde spin enhances mantle removal, at least 4 close encounters are needed to deplete Mercury mantle to present-day level.

Here we use N-body simulations of terrestrial planet formation to find out whether close encounter between proto-Mercury and proto-Venus occurs. We focus on those extreme encounters which can potentially lead to mantle removal of proto-Mercury. We describe our simulations and present our results in section 2 and section 3. Discussion follows in section 4. We then conclude in section 5.

2 SIMULATIONS

We used the *Mercury6* package to integrate the planetary embryo system assuming perfect merging upon collisions (Chambers 1999). We chose the confined annulus model of Hansen (2009) because of its high success rate in producing

Mercury analogues (Clement et al. 2019). This model is chosen also because of its simplicity requiring no extra parameters, unlike for example, parameters for the giant planet migration in the Grand Tack model (Walsh et al. 2011). Initially, the system consists of 400 planetary embryos of equal mass, $0.005 M_{\oplus}$ (Earth mass) placed between 0.7-1 au representing a flat surface density profile (Hansen 2009). The density of planetary embryos is assumed to be 4 g/cm^3 . Jupiter is placed at 5 au with eccentricity = 0.05. We used a timestep of 4 days (Hansen 2009; Lykawka & Ito 2017) and integrated the system for 200 million years (Clement et al. 2019; Kaib & Cowan 2015).

We carried out 250 simulations starting from different realisations of the above solids distribution (Hansen 2009). The evolution of this system is well documented in Hansen (2009) and here we focus on close encounters between Mercury and Venus analogues. At the end of simulations, the large bodies close to 0.7 au and 1 au are identified as Venus and Earth analogues. We note that we exclude systems left with only one dominant body (typically $> 1.33M_{\oplus}$) and three bodies (typically all larger than $0.33M_{\oplus}$) in later analysis. We formed 39 Mercury analogues ($a < 0.65 \text{ au}$ and $M < 0.2M_{\oplus}$) and 135 Mars analogues ($a > 1.3 \text{ au}$ and $M < 0.2M_{\oplus}$) in systems with Venus and Earth analogues clearly identified.

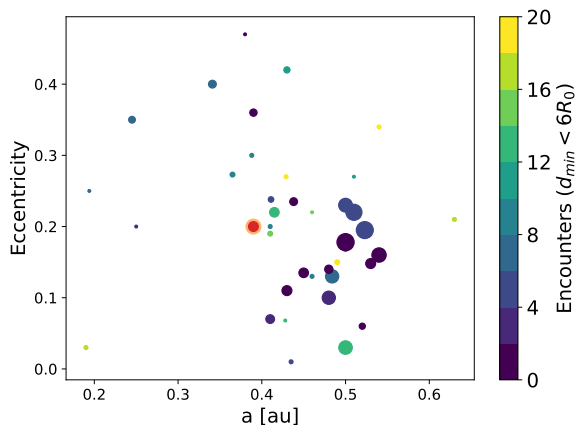


Figure 2. Orbital parameters of formed Mercury analogues. The plot consists of 39 Mercury analogues with the Mercury planet indicated by the red circle (the enlarged orange circle indicates a hypothetical chondritic Mercury). The area of the circles scales linearly with the mass of the objects while the color represents their times of major encounters with proto-Venus whose $d_{min} < 6R_0$ (see Figure 1). We note that Mercury analogues with masses larger than 0.3 Mercury mass have inclinations ($5^\circ - 13^\circ$) close to present-day Mercury inclination, 7° .

3 RESULTS

Hansen (2009) has already noted the orbital overlaps between proto-Mercury and proto-Venus in the early stage of planetary accretion (see Figure 6 of Hansen 2009). However, no details about proto-Mercury and proto-Venus encounters are reported therein. All our formed Mercury analogues are scattered inwards by proto-Venus. This is not surprising as the potential well is deep in the inner solar system and thus violent encounters are necessary to shrink proto-Mercury’s orbit. In figure 1, we show the encounter statistics between proto-Mercury and proto-Venus in a typical run. Both Mercury (green curve) and Venus (red curve) analogues accumulate materials quickly and are nearly fully-fledged at 40 Myr. Subsequently, a series of close encounters scatter proto-Mercury inside of proto-Venus. Here we focus on encounters after proto-Venus gains 0.7 Venus mass which can potentially remove proto-Mercury’s mantle (Deng 2020). We term these events as major encounters. Mass transfer in extreme close encounters can also happen between low mass embryos but ignored here because of the lack of available systematic studies.

In the exemplary run of figure 1, major encounters have a relative velocity at infinity $v_\infty \sim 10$ km/s. In major encounters, v_∞ shows no correlation with the closest approach, d_{min} which is typical of our simulations. The value of v_∞ ranges from 2 km/s to 10 km/s for major encounters in our simulations. The frequency of major encounter scales with the square of d_{min} when d_{min} is sufficiently large simply reflecting the geometric cross section scaling. We note that all encounters with d_{min} smaller than three Hill radii are recorded in our simulations. The occurrence rate of major encounter with d_{min} smaller than $10R_0$ (Venus radius, R_0) is rather irregular so that a statistical study is desirable.

We plot in figure 2 the orbital parameters of all the

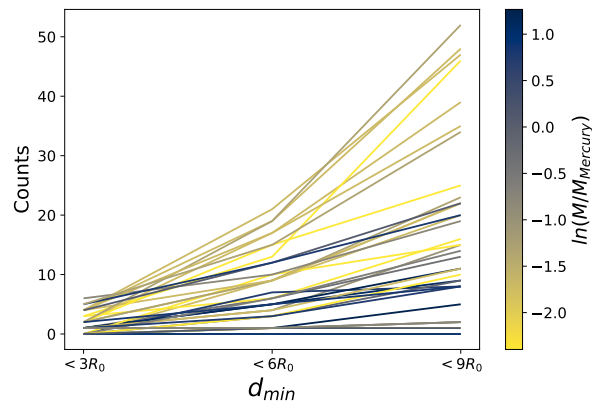


Figure 3. The number of proto-Mercury and proto-Venus major encounters (see Figure 1) with $d_{min} < 3R_0, 6R_0, 9R_0$ respectively. The line colors indicate the mass of the formed Mercury analogues in logarithmic scale. The median of encounter number for $d_{min} < 3R_0, 6R_0, 9R_0$ are 1, 6, 13 respectively.

Mercury analogues. The small Mercury analogues show large scatter in both the semi-major axis and eccentricity. However, there is a clustering of Mercury analogues around 0.5 au and eccentricity = 0.2. This group of Mercury analogues are more massive than Mercury or even a chondritic Mercury (a hypothetical Mercury with iron silicate mass ratio equals to 3:7). They also lie too close to Venus analogues (see also Clement et al. 2019, Figure 2). However, they are in line with the tidal mantle stripping model of Deng (2020) as mass transfer to Venus analogues (due to tidal interaction but ignored in N-body simulations) tends to shrink Mercury analogue’s semi-major axis towards present-day Mercury value, 0.39 au. The remaining question is whether these encounters are frequent and violent enough to remove proto-Mercury’s mantle significantly.

We calculated the number of extreme major encounters with d_{min} smaller than certain values ($3R_0, 6R_0, 9R_0$). It is noteworthy that Venus is able to deflect the orbit of a chondritic Mercury by 1° when $d_{min} = 9R_0$ and $v_\infty = 10$ km/s in a test hydrodynamic simulation similar to those of Deng (2020). In figure 3, the lighter Mercury analogues experienced more extreme major encounters in general. Three Mercury analogues (0.27, 0.45, 2.18 Mercury mass) have more than 4 (5, 6, 5) major encounters with $d_{min} < 3R_0$. We do not simply take them as successful realisations of the tidal mantle stripping hypothesis of Deng (2020) (see section 4). The median of encounter number for $d_{min} < 3R_0, 6R_0, 9R_0$ are 1, 6, 13 respectively. Extreme major encounters can dissipate orbital energy and even lead to mass transfer (Deng 2020). Our encounter statistics necessitate proper treatment of tidal interaction in the study of Mercury formation.

We may wonder why Mars is not metal enriched as Mercury. Beyond 1 au, the potential well is shallow so moderate encounters can already scatter Mars from ~ 1 au to 1.5 au. We carried out similar major encounter analysis for 39 randomly chosen Mars analogues (the trend does not change when more samples are included). In figure 5, we find only about 1 major encounter at $d_{min} < 9R_0$ between proto-Earth

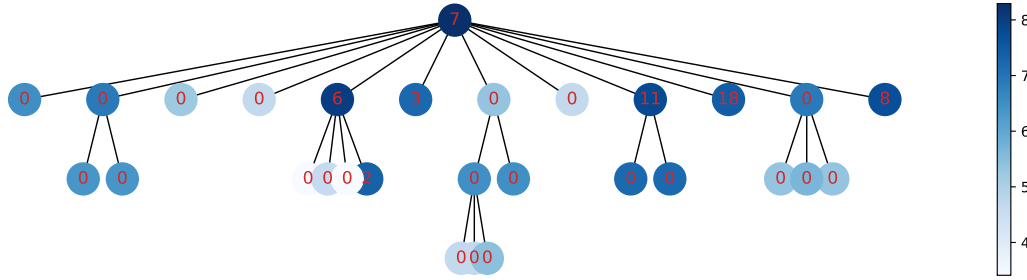


Figure 4. The merger and encounter history of a Mercury analogue of 0.11 Earth mass. The number label the times of major encounter with proto-Venus whose $d_{min} < 6R_0$ while the color represents the life time of embryos in logarithmic scale, i.e., \log (life time in years).

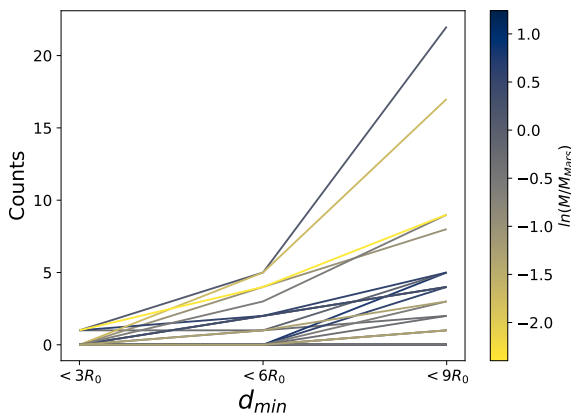


Figure 5. The number of proto-Mars and proto-Earth major encounters similar to figure 3. The median of encounter number for $d_{min} < 3R_0, 6R_0, 9R_0$ are 0, 0, 1 respectively.

and proto-Mars. Most major encounters have d_{min} tens of R_0 and $v_{\infty} \sim 5$ km/s. In some cases, Mars orbit can even diffuse outwards by indirectly exchanging angular momentum with proto-Earth through smaller objects (Hansen 2009).

4 DISCUSSION

We have shown clear evidence of extreme major encounters between proto-Mercury and proto-Venus in N-body simulations of terrestrial planet formation. We refrain from concluding on the probability of proto-Mercury mantle stripping (Deng 2020). During planetary accretion, extreme encounters happen between Mercury-Venus pairs of different masses, v_{∞} , d_{min} and spin. The parameter space explored by Deng (2020) is limited to $v_{\infty} < 3$ km/s and $d_{min} < 2R_0$ so results therein are not fully applicable here. A simple classification of planetary close encounter outcomes based on the Roche radius would be imprudent as Deng (2020) clearly shows spins of planets make a huge different.

Aside from the limited knowledge in planetary encounters (due to the high dimensional parameter space), we have not considered all interactions between proto-Mercury and proto-Venus in our analysis above. In figure 1, we only focus on the two objects bearing the identity of the final Mercury and Venus analogues. Embryos merged into the final Mercury analogue may have experienced extreme encounter with

proto-Venus as well. In figure 4, we demonstrate the growth and major encounter with proto-Venus for a Mercury analogue. Indeed, some embryos experience major encounters with proto-Venus and then merge into the final Mercury analogue. In this sense, the encounter times discussed above is a lower limit for the study of tidal mantle stripping.

On the other hand, the encounter statistics may not be accurate themselves. As we noted above, tidal dissipation at major encounters tends to bring proto-Mercury closer to proto-Venus (Deng 2020). We expect more encounters at smaller d_{min} if the dissipation caused by tidal interaction (wave excitation and/or mass transfer) is considered. Hybrid N-body and hydrodynamic simulations are necessary to address the formation of Mercury self-consistently.

The low v_{∞} in Mercury-Venus encounters casts further doubt on the single hit-and-run giant impact scenario for Mercury formation which requires a typical impact velocity $v_{imp} \sim 20$ km/s (Asphaug & Reufer 2014; Chau et al. 2018). Multiple impacts scenario at lower v_{imp} may reconcile with the observation of moderate volatiles on Mercury more easily than a single impact (Chau et al. 2018). However, repeatedly hit-and-run collisions between proto-Venus and proto-Mercury are much less likely than repeatedly close encounters out of simple geometric cross section consideration.

5 CONCLUSION

We carried out 250 N-body simulations of terrestrial planet formation. We found frequent close encounters between proto-Mercury and proto-Venus after the latter gained 0.7 Venus mass. About 13 such encounters have closest approach smaller than 9 Venus radii. These encounters scatters proto-Mercury to the innermost solar system. However, the formed Mercury analogues have a slightly larger semi-major axis (0.5 au) than present day Mercury value (0.39 au). We expect tidal orbital decay to lead to more violent encounters which eventually remove proto-Mercury’s mantle significantly and bring it further inward.

ACKNOWLEDGEMENT

H.D. acknowledge support from the Swiss National Science Foundation via an early postdoctoral mobility fellowship. We are grateful to comments from Sean Raymond on an

early version of this paper which lead to significant improvements. We thank the referee, John Chambers, for his report which greatly improved the clarity of the paper.

REFERENCES

- Anderson J. D., Colombo G., Esposito P. B., Lau E. L., Trager G. B., 1987, *Icarus*, 71, 337
- Asphaug E., Reufer A., 2014, *Nature Geoscience*, 7, 564
- Batygin K., Laughlin G., 2015, *Proceedings of the National Academy of Sciences*, 112, 4214
- Benz W., Anic A., Horner J., Whitby J. A., 2008, in , *Mercury*. Springer, pp 7–20
- Chambers J. E., 1999, *Monthly Notices of the Royal Astronomical Society*, 304, 793
- Chambers J., 2001, *Icarus*, 152, 205
- Chambers J., Wetherill G., 1998, *Icarus*, 136, 304
- Chau A., Reinhardt C., Helled R., Stadel J., 2018, *The Astrophysical Journal*, 865, 35
- Clement M. S., Kaib N. A., Raymond S. N., Walsh K. J., 2018, *Icarus*, 311, 340
- Clement M. S., Kaib N. A., Chambers J. E., 2019, *The Astronomical Journal*, 157, 208
- Deng H., 2020, *The Astrophysical Journal*, 888, L1
- Drazkowska J., Alibert Y., Moore B., 2016, *Astronomy & Astrophysics*, 594, A105
- Hansen B. M., 2009, *The Astrophysical Journal*, 703, 1131
- Hauck S. A., et al., 2013, *Journal of Geophysical Research: Planets*, 118, 1204
- Ida S., Lin D. N. C., 2008, *The Astrophysical Journal*, 673, 487
- Kaib N. A., Cowan N. B., 2015, *Icarus*, 252, 161
- Kokubo E., Ida S., 1998, *Icarus*, 131, 171
- Kokubo E., Ida S., 2000, *Icarus*, 143, 15
- Lykawka P. S., Ito T., 2017, *The Astrophysical Journal*, 838, 106
- Lykawka P. S., Ito T., 2019,] 10.3847/1538-4357/ab3b0a, 883, 130
- Morbidelli A., et al., 2016, *Icarus*, 267, 368
- Morishima R., Stadel J., Moore B., 2010, *Icarus*, 207, 517
- O’Brien D. P., Morbidelli A., Levison H. F., 2006, *Icarus*, 184, 39
- Peplowski P. N., et al., 2011, *science*, 333, 1850
- Raymond S. N., Izidoro A., 2017, *Science advances*, 3, e1701138
- Raymond S. N., O’Brien D. P., Morbidelli A., Kaib N. A., 2009, *Icarus*, 203, 644
- Raymond S. N., Izidoro A., Bitsch B., Jacobson S. A., 2016, *Monthly Notices of the Royal Astronomical Society*, 458, 2962
- Safronov V. S., 1969, *Evoliutsiia doplanetnogo oblaka*.
- Testi L., et al., 2014, *Protostars and Planets VI*, 914, 339
- Walsh K. J., Morbidelli A., Raymond S. N., O’Brien D. P., Mandell A. M., 2011, *Nature*, 475, 206

This paper has been typeset from a $\text{\TeX}/\text{\LaTeX}$ file prepared by the author.